# MONITORING AND EVALUATION OF A DIRECT COUPLED PHOTOVOLTAIC PUMPING SYSTEM

G. G. Merino, L. O. Lagos, J. E. Gontupil

**ABSTRACT.** *In this research, a direct coupled photovoltaic (DCPV) pumping system has been monitored and evaluated in order to assess energy losses due to mismatching between the photovoltaic (PV) array and the pump motor and to identify the errors associated with traditional procedures used for PV system sizing. The pumping system under study included a 12VDC, 94W PV module and a 12VDC, 7A, positive displacement 3-chamber diaphragm pump. The most common sizing method for this kind of system uses the monthly average of daily solar radiation to estimate energy generated and water pumped. To assess the above mismatching and errors, the actual PV energy converted to mechanical work in the PV pumping system was compared to the hypothetical energy converted by the system when working at the maximum power point (MPP), and to the theoretical energy predicted by the equations commonly used to size PV systems. The PV pumping system was installed at University of Concepcion in the central part of Chile and a data acquisition system was designed and implemented to measure the energy generated and water pumped. Analysis of 17 days of data showed that the most common sizing method for PV pumping systems estimated that only 84% of the energy would be available compared to operating the PV array at its maximum power point. Additionally, the most common sizing method overestimated by 15% the energy converted into useful work by the load.*

***Keywords.*** *Photovoltaic, PV pumping, Directly coupled, Monitoring.*

In Chile there are still about 540,000 rural families without electricity. The government goal is to provide electricity to at least 95% of the country by the year 2010. To this end, a rural electrification program is underway using photovoltaic (PV) technology, with about 2,400 PV systems already installed. One of the benefits of PV systems is that they can provide, in addition to illumination, electricity for water pumping, especially during the summer when more water is needed and when higher levels of solar radiation are available.

Photovoltaic pumping systems are especially suited to supply irrigation water in areas where the electrical grid is not available. Their main advantages over combustion engine pumps include practically zero maintenance, a long useful life, no fuel required for operation, no air contamination, and straightforward installation. Their principal disadvantage is a high capital cost.

Since 1978, the PV pumping market has being consistently growing. Some studies indicate more than 10,000 PV pumping systems in operation in the world by 1994 and predict about 50 times this figure for 2010 (Navarte et al., 2000).

Even though the average manufacturing cost of PV modules was reduced by 29% from 1992 to 1998 (Witt et al., 2001), the costs of small PV pumping systems are very high in Chile. Depending on the dealer, the price varies between $10 and $13 (US) per peak watt. Considering these prices, the methodology used to size PV systems must be accurate enough to avoid over-sizing or under-sizing, which can make the system unnecessarily expensive or cause it to not meet user expectations, respectively.

The size of a PV system is strongly dependent upon the energy requirement of the loads which are to be served. The electrical energy output of the system is determined by solar radiation, ambient temperature, and also by the interaction between the PV modules and the load. PV module data specifications provided by manufacturers are essential for the design and sizing of a solar array (Taha, 1995). Traditional methods to design these systems use monthly averages of daily accumulated radiation (Alonso and Chenlo, 1992; Strong and Scheller, 1993; Sandia National Laboratories, 1995; Markvart, 1996; Cuadros et al., 2004). Since the energy output from a PV module is affected by others factors in addition to solar radiation, these approaches do not guarantee a design that optimizes the size of these devices. Additionally, power ratings of PV devices do not usually give an accurate indication of their outdoor performance. Dyk et al. (2002) provided evidence that meteorological conditions could cause an 18% reduction of a module's potential power.

The least expensive method of pumping water using PV energy is directly connecting a DC motor, which drives the pump, to a PV array without batteries. The theory of direct coupling between DC motors and PV units is well documented in the literature (Appelbaum and Bany, 1979;

Submitted for review in March 2007 as manuscript number PM 6938; approved for publication by the Power & Machinery Division of ASABE in March 2008.

Mention of a vendor does not imply endorsement over other vendors.

The authors are **Gabriel Guillermo Merino,** Professor, Departamento de Mecanizacion y Energia, Universidad de Concepcion, Chillan, Chile; **Luis Octavio Lagos, ASABE Member,** Ph.D. Student, University of Nebraska, Lincoln, Nebraska; and **Jorge Esteban Gontupil,** M.S. Student, Departamento de Mecanizacion y Energia, Universidad de Concepción, Universidad de Concepcion, Chillan, Chile. **Corresponding author:** Gabriel Guillermo Merino, Departamento de Mecanizacion y Energia, Universidad de Concepcion, Chillan, Chile, Avenida Vicente Mendez 595; phone: 56-42-208818; fax: 56-42-275303; e-mail: gmerino@udec.cl.

  ISSN 0883-8542

Roger, 1979; Appelbaum, 1981; Townsend, 1989; Akbaba et al., 1998; Abidin and Yesilata, 2004). For a given solar radiation incident on the modules and a given cell temperature, there is a unique point in the current-voltage (I-V) curve of the PV array at which the electrical power output is maximum; the maximum power point (MPP). In figure 1, the characteristic I-V curve and power curve for the PV module used in the system analyzed in this work are shown. Most DC motors can operate far from the MPP at most radiation levels and temperatures. The point on the I-V curve where the system is operating (operation point) is determined by the intersection of the PV module I-V curve and the load I-V curve. Thus, an electrical mismatch could occur between the I-V characteristics of the motor and the I-V characteristics of the PV array. To minimize this problem the DC motor and the pump must be carefully selected to match as close as possible the maximum power trajectory of the PV array (Saied, 1988; Saied and Jaboori, 1989). Unfortunately, most of the time, the load I-V curve is not provided by the load manufacturer.

An alternative to the direct-coupled PV system is a battery-buffered PV pumping system, where a battery is connected across the PV array and the DC motor through a voltage regulator. With this configuration a constant voltage is provided to the motor independent of the solar radiation available. Another possibility is to consider a maximum power point tracker (MPPT). In this case a DC-DC converter continuously matches the MPP characteristics of the PV array to the input characteristics of the DC motor that drives the pump (Calais and Hinz, 1998). The two options however, add more cost and complexity to the system and therefore, the tradeoff between higher energy conversion efficiency and higher installation costs must be assessed.

The main objective of this work was to compare the actual PV energy converted to mechanical work in a direct coupled PV pumping system to the hypothetical energy converted by the system when working at the MPP, and to the theoretical energy generated as predicted by the equations commonly used to size PV systems. To this end, a photovoltaic module was connected directly to a DC motor and pump and a data acquisition system was set up to measure in real time the power flow between the system components (fig. 2). The hypothetical energy generated by the photovoltaic module

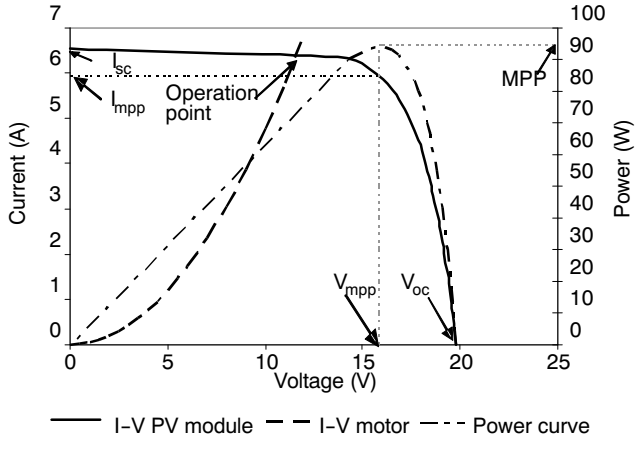


**Figure 1. Current-voltage (I-V) curves for the PV module and load, and the PV module power curve.**

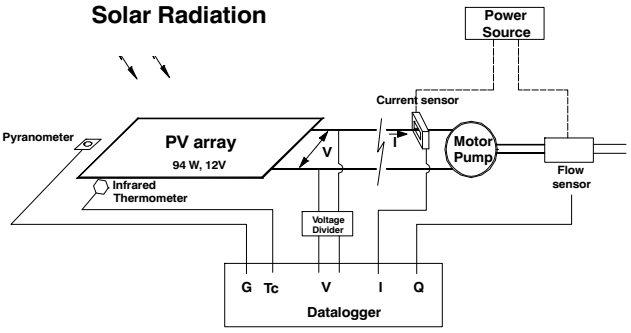


**Figure 2. Layout of the photovoltaic pumping system and data acquisition system.**

when working at its MPP was estimated using an electrical model that simulated the PV module and its MPP according to the actual solar radiation and PV module temperature which were measured by the data acquisition system. The study was performed at the Universidad de Concepción which is located in the central region of Chile.

## SIZING PV-PUMPING SYSTEMS

The common PV system design methods are based on an energy balance between the solar energy available on the site and the daily energy required by the load, $E_{load}$ (Wh day$^{-1}$) (Sandia National Laboratories, 1995; Markvart, 1996). The number of modules needed in the PV array is calculated based on the ratio between the daily accumulated current required for the load $I_{load}$ (Ah day$^{-1}$) and the daily accumulated current generated by a single PV module $I_a$ (Ah day$^{-1}$). $I_{load}$ can be expressed as:

$$I_{load} = \frac{E_{load}}{\eta \cdot V_n} \quad (1)$$

where $\eta$ is the wire loss factor and $V_n$ is the system's nominal voltage. On the other hand and according to most design handbooks (Alonso and Chenlo, 1992; Strong and Scheller, 1993; Sandia National Laboratories, 1995; Markvart, 1996), $I_a$ can be estimated as:

$$I_a = PSH \cdot I_{mpp} \quad (2)$$

where the peak solar hours (PSH) is the equivalent number of hours per day at reference irradiance (1000 Wm$^{-2}$) which equal the same accumulated daily radiation as the actual radiation levels distributed through the day. The current, $I_{mpp}$, is the current generated by the photovoltaic module when working at MPP under reference conditions (1000 W m$^{-2}$ of radiation incident on the PV module and cell temperature of 25°C). The previous equations allow the designer to size the PV array to meet the required daily accumulated current. However, the PV module temperature depends strongly on the ambient air temperature, wind speed, and solar radiation. With light winds and 1000 Wm$^{-2}$ of radiation at the module plane, and air temperatures around 40°C, a module can reach a temperature of 70°C or higher (Posorski, 1996). Some causes of this rise in temperature are: the non-active absorption of photons, the recombination of

electron-hole pairs, photocurrent (Joule's effect), and parasitic currents. The cell temperature deviations above the standard condition temperature (25°C) increase the lattice vibration, leading to electron-photon scattering, reducing the mobility of charge carriers and reducing the built-in p-n junction voltage. The overall effect is a reduction of the module maximum output power by about 0.66% per °C of temperature increase (Radziemska, 2003). Equations 1 and 2 do not take this phenomenon into account and therefore they would over-estimate the daily current generated by the PV array.

## Current-Voltage Curve and Modeling a PV Module

An assessment of the operation of solar cells and the design of power systems based on solar cells must be based on their electrical characteristics, i.e., the voltage-current relationships of the cells under various levels of radiation and cell temperatures.

### The Photovoltaic Module

There are several models in the literature to simulate the behavior of a PV cell or module. The degree of complexity of the model will determine which method is more suitable for extracting the model parameters (Blas et al., 2002). In this work, the model used to describe the electrical behavior of the PV module is represented by the single diode equivalent circuit shown in figure 3. This model allows simulating the PV cell behavior with a sufficient degree of precision and at the same time allows calculating the model parameters in a straight forward manner (Townsend, 1989).

This circuit requires four parameters to be known: the light current, $I_L$, the diode reverse saturation current, $I_o$, the series resistance, $R_s$, and a curve fitting parameter, a. For a given cell temperature, $T_c$, and solar radiation incident on the PV module, $G_T$, the current-voltage curve relationship characteristic of this model is given by

$$I = I_L - I_D = I_L - I_o\left[\exp\left(\frac{V + I \cdot R_s}{a}\right) - 1\right] \qquad (3)$$

The power generated by the PV module can be estimated by

$$P = I \cdot V \qquad (4)$$

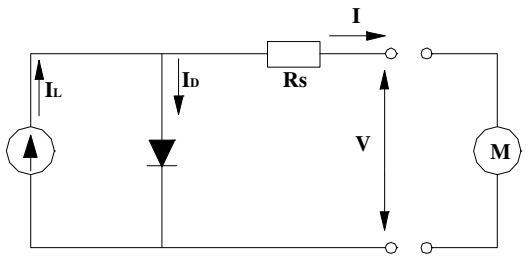


**Figure 3. Equivalent circuit used to simulate the photovoltaic module.**

The point where the curve cuts the current axis (where $V = 0$) is the short circuit current, $I_{sc}$, and the intersection with the voltage axis (where $I = 0$) is the open circuit voltage, $V_{oc}$. At maximum power point (MPP) the power is $P_{mpp}$, the current is $I_{mpp}$, and the voltage is $V_{mpp}$. Ideally, cells would always operate at maximum power point, but practically cells operate at a point on the *I-V* curve that matches the *I-V* characteristic of the load.

In this model the series resistance $R_s$ is assumed to be independent of temperature (Townsend, 1989). Here we use the methodology given by Duffie and Beckman (1991) to calculate the model parameters. The following equations describe the method used to determine those parameters:

$$R_s = \frac{a \cdot \ln\left(1 - \frac{I_{mpp}}{I_L}\right) - V_{mpp} + V_{oc}}{I_{mpp}} \qquad (5)$$

$$\frac{a}{a_{ref}} = \frac{T_c}{T_{c_{ref}}} \qquad (6)$$

$$I_L = \frac{G_T}{G_{Tref}}\left[I_{Lref} + \mu_{ISC}\left(T_c - T_{c\,ref}\right)\right] \qquad (7)$$

$$\frac{I_o}{I_{o\,ref}} = \left(\frac{T_c}{T_{c\,ref}}\right)^3 \exp\left[\frac{\varepsilon \cdot N_s}{a_{ref}}\left(1 - \frac{T_{c\,ref}}{T_c}\right)\right] \qquad (8)$$

where ε is the material band gap energy, 1.12 eV for silicon, and $N_s$ is the number of cells in series in a module times the number of modules in series. All of the quantities with the subscript "ref" are from measurements at reference conditions (1000 W $m^{-2}$ incident radiation and 25°C cell temperature).

Knowing the temperature coefficient of the short circuit current, $\mu_{ISC}$, and the temperature coefficient of the open circuit voltage, $\mu_{VOC}$, it is possible to evaluate the fourth model parameter, a, by combining the equations 6 and 9:

$$a_{ref} = \frac{\mu_{VOC} \cdot T_{c\,ref} - V_{oc\,ref} + \varepsilon \cdot N_s}{\frac{\mu_{ISC} \cdot T_{c_{ref}}}{I_{Lref}} - 3} \qquad (9)$$

Measurements at the reference condition of $V_{oc}$, $I_{sc}$, $I_{mpp}$, $V_{mpp}$, $\mu_{ISC}$, and $\mu_{VOC}$, as provided by the manufacturer, are used to determine $I_L$, $I_o$, $R_s$, and $a$ at the reference condition. These are then used to determine $I_L$ and $I_o$ at any cell temperature. Finally, the current-voltage-power characteristics are then determined for any specific cell temperature and radiation level.

### Current and Voltage at Maximum Power Point

In order to obtain the current and voltage at MPP for a specific radiation and cell temperature, it is possible to differentiate the equation for power (eq. 4) with respect to $V$ and set the result equal to zero. The result is a transcendental equation that must be solved numerically:

$$I_{mpp} + \frac{\left(I_{mpp} - I_L - I_o\right)\left[\ln\left(\frac{I_L - I_{mpp}}{I_o} + 1\right) - \frac{I_{mpp} \cdot R_s}{a}\right]}{1 + \left(I_L - I_{mpp} + I_o\right)\frac{R_s}{a}} \quad (10)$$

$$= 0$$

A value of $I_{mpp}$ can be obtained numerically from equation 10, and then using equations 3 and 4, voltage at maximum power point and maximum power can be calculated for any cell temperature at any value of radiation.

## Experimental Setup

A direct coupled PV pumping system (fig. 2) was installed outdoors at the University of Concepción, Chile, Campus Chillán, 36°32' South latitude, 72°06' West longitude, at 144 m above sea level. The system was monitored from 14 January to 14 February 2007. The energy generated and power flows were measured with a data acquisition system at regular intervals and used to evaluate the performance of the system. The panel was mounted at a tilt angle of 15° and oriented to magnetic North. Pumping water was recycled into a storage tank assuring availability during high radiation periods. Detailed information related to systems components are provided in table 1.

**Table 1. Description of pumping system components.**

| | |
|---|---|
| PV module: I-94 (Isofotón, Malaga, Spain) | |
| Standard test conditions | |
| Nominal voltage | 12 V |
| Open circuit voltage ($V_{oc}$) | 19.8 V |
| Voltage at MPP ($V_{mpp}$) | 16 V |
| Short circuit current ($I_{sc}$) | 6.54 A |
| Current at MPP ($I_{mpp}$) | 5.88 A |
| Cell temperature coefficients | |
| Temp. coefficient of the short circuit current ($\mu_{ISC}$) | 0.00275 A°C$^{-1}$ |
| Temp. coefficient of the open circuit voltage ($\mu_{VOC}$) | -75.9 mV°C$^{-1}$ |
| Module features | |
| Number of cells in series in one module | 33 |
| Number of cells in parallel | 2 |
| Length | 1208 mm |
| Width | 654 mm |
| Thickness | 39.5 mm |
| Cost[a] | US$940 |
| DC pump, model: 2088-423-344 ( SHURflo, Cypress, Calif.) | |
| Open flow | 10.6 L min$^{-1}$ |
| Pressure | 3.1 Bar |
| Nominal voltage | 12 V |
| Nominal current | 7 A |
| Cost[a] | US$350 |

[a] Costs were obtained in 2007.

### Data Acquisition System

Data acquisition systems (DAS) are widely used in renewable energy source applications (Benghanem et al., 1999; Koutroulis and Kalaitazakis, 2003) to collect data on installed system performance. In this research, a DAS was used to monitor the performance of the photovoltaic water pumping system. The solar radiation on the inclined PV module (W m$^{-2}$) was measured with a pyranometer LI-200 (LI-COR Biosciences, Lincoln, Neb.). Temperature of the PV panel, which was assumed to be equal to the cell temperature, was measured with a digital infrared thermometer Heat Spy(Wahl Instruments, Long Branch, N.J.) with an accuracy of ±1°C and an output signal scaled to 1 mV/°C. Voltage of the array was measured using a voltage divider with an output voltage of 0.15 V/V in the PV module. The DC current was measured with a non-intrusive Hall Effect type current transducer HAS 50-S(LEM, Geneva, Switzerland), output voltage ±4V ±40mV, supply voltage ±15V. Flow rate was measured with a flow transducer, model: 257-133 (RS, Madrid, Spain), range 1.5-30 L min$^{-1}$, output signal 1200 pulses L$^{-1}$ (max 600 Hz), supply voltage ±5V. The DAS was equipped with a power source unit (+15, -15, +5, -5, and 0 V) as source of voltage for the current and flow sensors. The DAS sampling rate was 1 Hz and values recorded were integrated and stored each 2 min in a micrologger CR21X(Campbell Scientific, Logan, Utah)

## Data Analysis and Results

Since each day of analysis required computer simulations with a time step of 2 min, to reduce the amount of data to be verified, 17 days were randomly selected from the 32 days of operation and data monitoring, analyzed, and reported in this article. For each day, current and voltage, incident radiation on the PV module, cell temperature, and flow rate were measured every second and integrated every 2 min. Figures 4 and 5 show, as an example, the parameters measured for two consecutive days.

### Electrical Circuit Model of the PV Module

To demonstrate how accurately the electrical circuit model simulates the behavior of the PV module, current-voltage curves provided by the manufacturer were compared with curves modeled by using equation 3. Figure 6 shows the comparison of the I-V characteristic curve of the PV module obtained from information provided by the manufacturer and the curve obtained with the one diode model. From this figure it is evident that the model has high accuracy.

### Daily Energy Generated by the PV Module

Daily energy generated by the PV module and converted by motor ($E_{est}$), was estimated following the traditional design method by using equations 1 and 2. In these equations $I_{load} = I_a$, $\eta = 1$. PSH was calculated using the daily accumulated irradiance measured by the pyranometer. On the other hand, the daily energy that could have been generated with the module operating at its maximum power point ($E_{mpp}$) was calculated by simulating the PV module through the day using the measured cell temperature, the measured solar radiation on the inclined plane, and the model

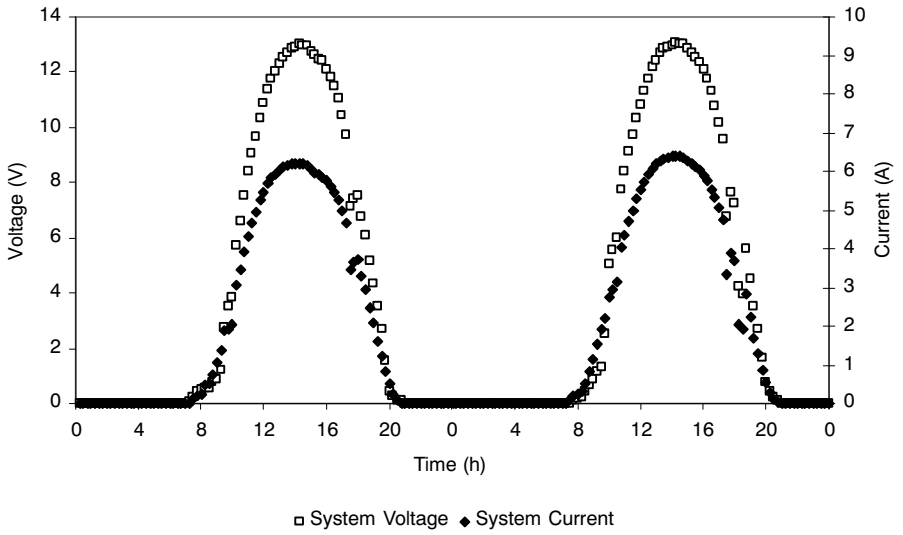


**Figure 4. System voltage and system current measured by the DAS over two days, during the summer of 2007.**

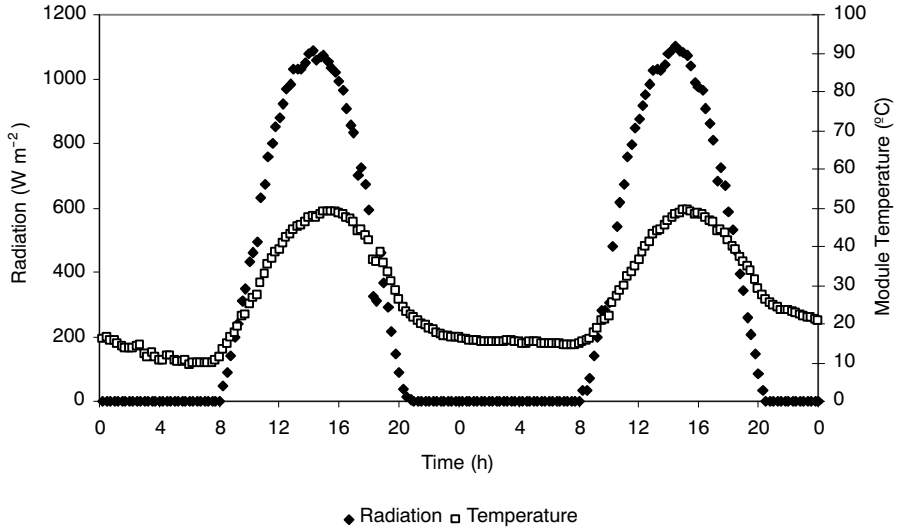


**Figure 5. Incident radiation on the PV module and module temperature measured by the DAS over two days.**

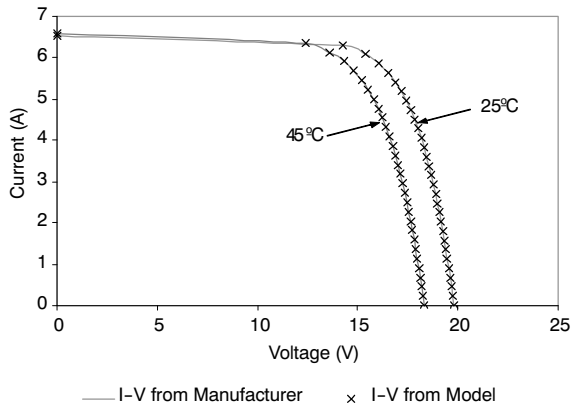


**Figure 6. I-V curves generated with the one diode model and those provided by the manufacturer at 1000 W m$^{-2}$ of incident solar radiation at PV cell temperatures of 25°C and 45°C.**

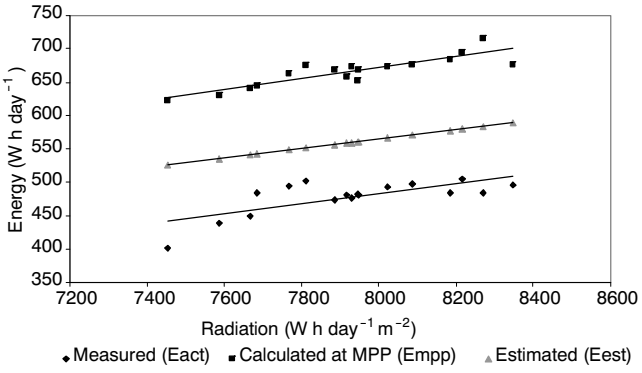


**Figure 7. Daily energy converted to useful work by the load ($E_{act}$), daily energy estimated by the design method ($E_{est}$) and daily energy calculated at MPP ($E_{mpp}$) for different daily accumulated radiation levels.**

developed for the PV module (eqs. 3 through 10). These equations were incorporated in Visual Basic code and solved using the bisection method. Figure 7 shows the daily energy estimated by the design method ($E_{est}$) and the daily energy calculated with the PV module operating at its MPP ($E_{mpp}$). This figure also shows the energy actually converted to useful work by the load as measured by the data acquisition system ($E_{act}$), for the 17 days reported in this work. In figure 7 the days were ordered according to the accumulated daily radiation along the abscissas and a regression line was added to each group of data.

The ratio $E_{est}/E_{mpp}$ was calculated for the 17 days analyzed. The energy estimated by the design method averaged 84% of the energy calculated at MPP (range 82% to 87%). To assess the causes of this difference, the daily accumulated current corresponding to the maximum power point $I_{mpp}$ and the daily accumulated current estimated by the design method $I_a$ were calculated and compared. Results indicated that the accumulated $I_a$ almost equaled the accumulated $I_{mpp}$ for every day. This is due to the fact that $I_{mpp}$ is not significantly affected by changes of temperature and it is directly related to radiation. Thus, the difference between the daily energy estimated by the design method and the daily energy calculated at MPP is caused by the variation of voltage $V_{mpp}$ with cell temperature and radiation. From the above, and in order to simplify the calculations of power at maximum power point, the current $I_{mpp}$ at any cell temperature and radiation can be estimated using a direct relationship between the current $I_{mpp}$ and radiation at standard condition through the equation:

$$I_{mpp} = I_{mpp\ ref} \frac{G_T}{G_{T\,ref}} \tag{11}$$

From this equation, $V_{mpp}$ and $P_{mpp}$ can be computed using equations 3 and 4. On the other hand, the difference between the daily energy estimated by the design method and the daily energy calculated at MPP is due to the fact that the system nominal voltage $V_n$ =12V is applied in equation 1. According to figure 7, in order to avoid this difference, $V_n$ needs to be replaced in equation 1 by a voltage approximately equal to 90% of the voltage at MPP calculated at reference conditions ($V_{mpp}$). In this case $V_{mpp}$ =16 V, therefore the voltage to be used in the design procedure needs to be about 14.4 V, if the system is forced to work in its MPP.

As previously indicated, during the operation of a PV system the load characteristics may not match the MPP of the PV array. In order to quantify the mismatch, the voltage and current measured by the DAS were used to calculate the actual energy converted to useful work by the load ($E_{act}$) during the day and these values were compared with $E_{mpp}$. The ratio $E_{act}/E_{mpp}$ was calculated for each of the seventeen days studied. Figure 7 shows the energy measured and the energy calculated at MPP for different radiation levels. The average energy converted to useful work by the system was 72% of the energy calculated at MPP (range 64% to 75%) without a clear dependency on the accumulated radiation. To illustrate this phenomena, figure 8 shows the current $I_{mpp}$ calculated and the load current measured for one day of data, where the average radiation during the day was 623 W $m^{-2}$ and the average cell temperature was 35.5°C (range 13°C to 48°C). In this figure it is possible to see the situation for a day with a high radiation level. The pumping system current follows the $I_{mpp}$ during the day but the system voltage deviates from the voltage ($V_{mpp}$) corresponding to the MPP. This explains the difference obtained between $E_{act}$ and $E_{mpp}$.

In order to understand pattern followed by the voltage during the day it is necessary to illustrate the electrical model (fig. 9) that describes the DC motor with permanent magnets which drives the pump (Cogdell, 1996).

The voltage ($V$) across the motor in steady state is related to the armature current ($I_a$), the armature resistance ($R_a$), and the armature emf ($E$):

$$V = R_a \cdot I_a + E \tag{12}$$

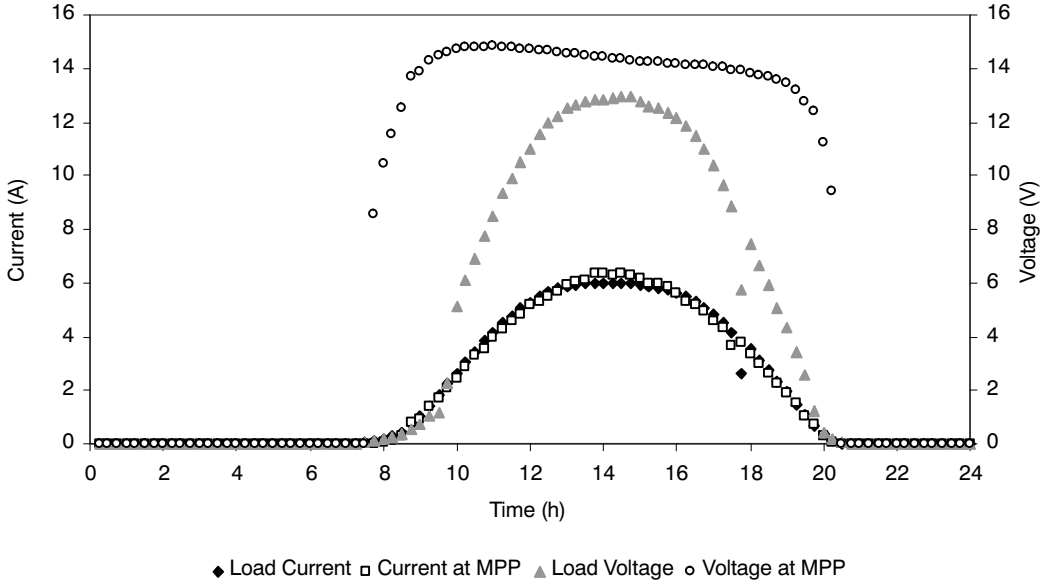


**Figure 8. Actual PV module current and voltage and simulated PV module current and voltage at maximum power point.**

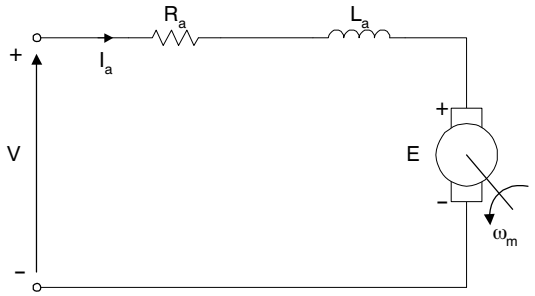


**Figure 9. Circuit model for the DC permanent magnet motor.**

By Faraday's law, the emf is proportional to flux ($\phi$), provided by the permanent magnets, and the rotation speed ($\omega_m$), and hence may be expressed by the relationship:

$$E = K_E \cdot \phi \cdot \omega_m \tag{13}$$

where $K_E$ is a constant that depends on rotor size, the number of rotor turns, and details of how these turns are interconnected. By Ampere's force law, the developed torque is proportional to armature current, and hence may be expressed as

$$T_m = K_T \cdot \phi \cdot I_a \tag{14}$$

where $K_T$ is a constant that also depends on rotor size, the number of rotor turns, and details of how these turns are interconnected. Conservation of energy requires that the constants in equations 13 and 14 be the same. On the other hand, if we assume the rotational-loss torque is constant or varies linearly with speed, the output torque will have the form of a straight line:

$$T_m(\omega) = C_1 - C_2 \cdot \omega_m \tag{15}$$

where $C_1$ and $C_2$ are constants.

From equations 14 and 15, a relationship between $\omega_m$ and $I_a$ can be obtained, and from this relationship we can obtain the relationship between $E$ and $I_a$. The result is that the voltage varies linearly with the armature current as:

$$V = R_a \cdot I_a + K_T \cdot \phi \left[ \frac{C_1 - K_T \cdot \phi \cdot I_a}{C_2} \right] \tag{16}$$

The linear relationship between motor voltage and motor current in equation 16 accounts for the voltage curve illustrated in figure 8 and explains why the system cannot operate at the MPP of the PV module.

To address this issue, a maximum power point tracker (MPPT) could be incorporated between the PV module and the motor. This device is a power electronic DC-DC converter inserted between the PV module and its load to achieve optimum matching. When using a MPPT the ratio of the input and output voltage is controlled by varying the on-off duty cycle of the converter switching device, typically a MOSFET. A number of tracker algorithms have been proven and used and a number of DC-DC converter topologies are possible. The inclusion of a MPPT into the PV pumping system will be addressed in the near future by the authors of this study.

In relation to the accuracy of the method used to size PV systems, over-sizing has been defined as the deviation of the actual energy converted to useful work by the load from the theoretical expected energy generated by the PV array per day (Taha, 1995). Over-sizing ($O$) can be calculated using the relation:

$$O = \frac{E_{est} - E_{act}}{E_{est}} \cdot 100 \tag{17}$$

where $E_{est}$ represents the theoretical daily expected energy generated by the PV module in $Whday^{-1}$, which can be calculated as $PSH \cdot I_{mpp} \cdot V_n$, and the $E_{act}$ is the daily measured energy converted by the load. Over-sizing calculated for 17 days averaged 14.6% (range: 9% to 24%) without a clear dependency on the daily accumulated radiation. There are two factors that generate the above difference between $E_{est}$ and $E_{act}$; the first one is the voltage used in equation 2. ($V_n$), the second is the mismatch between the electric load (the motor in this case) and the PV array as explained previously. To assess this problem, it is necessary to include in the system a MPPT device to force the PV module to be working at its MPP. If this is achieved, then $V_n$ can be replaced in equation 2 by $0.9V_{mpp}$ (calculated at reference conditions). By doing this the predicted energy by the design method will match the energy converted by the load.

## CONCLUSIONS

The one-diode model applied to simulate the current-voltage curves of the PV module under any condition of cell temperature and radiation agreed with the experimental curves provided by the manufacturer. The power and daily energy generated by the PV system gave a clear indication of the operational performance. The rated power of PV devices does not usually give an accurate indication of outdoor performance, as was seen in this analysis. Under actual field operating conditions a decrease in the PV module output as compared to the calculated value from the design method was the result of factors such as mismatch between load characteristics and the maximum power operating point of the PV module, temperature variation, and variation in solar radiation levels (instantaneous and total daily). The deviation of the operation point from the MPP is due to the fact that the system voltage does not follow the maximum voltage under a given solar radiation and cell temperature. To overcome this problem, a maximum power point tracker device can be incorporated into the system. The tradeoff between the additional costs associated with this device and the gain in useful energy will be addressed in future work.

This study showed that the traditional method of design for direct coupled PV systems estimated around 84% of the energy potentially available from the array and overestimated by 14.6% the energy converted to useful work by the load. The traditional method is a good tool to design systems, but more detailed methods are necessary to provide better approximations of the characteristics of the system. Thus, if the system is forced to follow the MPP then, during the design process, not the nominal system voltage but a voltage equal to 90% of the maximum power point voltage calculated at reference condition should be used to estimate the daily energy converted by the system.

**ACKNOWLEDGEMENTS**

The authors wish to acknowledge the financial support of the Fondo de Desarrollo para la Ciencia y la Tecnologia FONDECYT (project No. 1040506) Chile and the University of Concepcion.

## REFERENCES

Abidin, Z., and B. Yesilata. 2004. New approaches on the optimization of directly coupled PV pumping systems. *Solar Energy* 77(1): 81-93.

Akbaba, M., I. Qamber, and A. Kamal. 1998. Matching of separately excited dc motors to photovoltaic generators for maximum power output. *Solar Energy* 63(6): 375-385.

Alonso, M., and F. Chenlo. 1992. Chapter 19: Diseño y dimensionado de sistemas de bombeo fotovoltaico. In *Fundamentos, dimensionado y aplicaciones de la energía solar fotovoltaica*, 19.1-19.45. Madrid, España: CIEMAT.

Appelbaum, J., and J. Bany. 1979. Performance analysis of D.C. motor-photovoltaic converter system-I. *Solar Energy* 22(5): 439-445.

Appelbaum, J. 1981. Performance analysis of D.C. motor-photovoltaic converter system-II. *Solar Energy* 27(5): 421-431.

Benghanem, M., A. Hadj Arab, and K. Mukadam. 1999. Data acquisition system for photovoltaic water pumps. *Renewable Energy* 17(3): 385-396.

Blas, M. A., J. L. Torres, E. Prieto, and A. García. 2002. Selecting a suitable model for characterizing photovoltaic devices. *Renewable Energy* 25(3): 371-380.

Calais, M., and H. Hinz. 1998. A ripple-based maximum power point tracking algorithm for a single-phase, grid-connected photovoltaic system. *Solar Energy* 63(5): 277-282.

Cogdell, J. R. 1996. *Foundations of Electrical Engineering*, 2nd ed. Upper Saddle River, New Jersey: Prentice Hall.

Cuadros, F., F. Lopez-Rodriguez, A. Marcos, and J. Coello. 2004. A procedure to size a solar-powered irrigation (photoirrigation) schemes. *Solar Energy* 76(4): 465-473.

Duffie, J. A., and W. A. Beckman. 1991. *Solar Engineering of Thermal Processes.* New York: John Wiley and Sons.

Koutroulis, E., and K. Kalaitazakis. 2003. Development of an integrated data-acquisition system for renewable energy sources systems monitoring. *Renewable Energy* 28(1): 139-152.

Markvart, T. 1996. *Solar Electricity.* Chichester, England: John Wiley and Sons.

Navarte, L., E. Lorenzo, and E. Caamaño. 2000. PV pumping analytical design and characteristics of boreholes. *Solar Energy* 68(1): 49-56.

Posorski, R. 1996. Photovoltaic water pumps, an attractive tool for rural drinking water supply. *Solar Energy* 58(4-6): 155-163.

Radziemska, E. 2003. The effect of temperature on the power drop in crystalline silicon solar cells. *Renewable Energy* 28(1): 1-12.

Roger, J. A. 1979. Theory of the direct coupling between D.C. motors and photovoltaic solar arrays. *Solar Energy* 23(3): 193-198.

Saied, M. M. 1988. Matching of DC motors to photovoltaic generators for maximum daily gross mechanical energy. *IEEE Trans. Energy Conversion* EC-3: 465-472.

Saied, M. M., and M. G. Jaboori. 1989. Optimum solar array configuration and dc motor field parameters for maximum annual output mechanical energy. *IEEE Trans. Energy Conversion* EC-4: 459-465.

Sandia National Laboratories. 1995. Stand-alone photovoltaic systems. A handbook of recommended design practices. Albuquerque, N.M.: Sandia National Laboratories.

Strong, S. J., and W. G. Scheller. 1993. *The Solar Electric House* . Still River, Mass.: Sustainability Press.

Taha, A. 1995. The oversizing method of estimation in PV systems. *Renewable Energy* 6(5-6): 487-490.

Townsend, T. U. 1989. A method for estimating the long-term performance of direct-coupled photovoltaic systems. MS thesis. Madison, Wis.: University of Wisconsin-Madison, Department of Mechanical Engineering.

van Dyk, E. E., E. L. Meyer, F. J. Vorster, and A. W. R. Leitch. 2002. Long-term monitoring of photovoltaic devices. *Renewable Energy* 25(2): 183-197.

Witt, C. E., R. L. Mitchell., H. P. Thomas, and M. S. Davies. 2001. Terrestrial photovoltaic technologies update. *Renewable Energy* 23(3-4): 349-353.